Observations of AGN with MIDI

Konrad R. W. Tristram

Max-Planck-Institut für Astronomie, Königstuhl 17, 69117 Heidelberg, Germany

Abstract

The capabilities of MIDI and the VLTI play a key role in the study of the central region of active galaxies, because the instrument (a) operates at the necessary wavelength range, namely the mid infrared, and because (b) it provides the necessary spatial resolution to analyse the circumnuclear dust distribution in these objects. The observations, however, turn out to be challenging due to the faintness of the sources, which are close to the sensitivity limit of MIDI. Nevertheless six objects have been observed successfully so far, more than originally anticipated. The faintness has implications for the data reduction, which can only be accomplished using the coherent data reduction package EWS. In spite of these challenges, MIDI has produced interesting results for the sources analysed: NGC 1068 and Circinus seem to confirm the picture of a geometrically thick dust distribution, while the nuclear MIR emission of Centaurus A appears to be mainly of non-thermal origin. The remaining objects are barely resolved and more data is needed to determine the properties of their dust emission.

Key words:
radiation mechanisms: thermal, techniques: interferometric, galaxies: Seyfert, galaxies: individual (NGC 1068, Circinus, Centaurus A, NGC 3783, MCG-05-23-01, Mrk 1239)

1 Introduction

In general, Active Galactic Nuclei (AGN) refer to outstanding energetic phenomena in the central regions of galaxies. These phenomena are interpreted to be manifestations of a supermassive black hole ($M > 10^6\,\mathrm{M}_\odot$) at the centre of a galaxy, which is accreting matter from the inner parsecs of its host. In the standard model, the so-called "unified scheme", the central engine, consisting

Email address: tristram@mpia.de (Konrad R. W. Tristram).

of a hot accretion disk around the black hole, is assumed to be surrounded by a geometrically thick distribution of gas and dust, the dusty torus. Such a configuration is thought to give a simple explanation for the dichotomy observed between Seyfert 1 and Seyfert 2 galaxies: type 1 objects are seen face-on, allowing a direct view towards the central engine, while type 2 objects are oriented edge-on, so that the dust in the torus blocks the line of sight towards the very centre. Initially, all arguments for the existence of such tori had to be based on theoretical considerations and on indirect observational evidence such as the spectral energy distributions (SED) of AGN. However, alternative pictures have been forwarded. It is argued for example that the presence of a warped disc, as detected in maser emission in several objects, is responsible for the properties of AGN.

Until recently it was not possible to explore the circumnuclear dust distribution directly due to the lack of angular resolution: even for the nearest AGN the expected structures are too small (on the order of a parsec and hence smaller than 100 mas) to be resolved by single dish telescopes in the mid infrared (MIR), where the dust emission is strongest. Only interferometry can provide the necessary angular resolution to directly test the torus paradigm or alternative explanations. As I will show, the MID-infrared Interferometric instrument (MIDI) at the Very Large Telescope Interferometer (VLTI) of the European Southern Observatory (ESO) on Cerro Paranal is by far the best instrument to implement this technique and to directly resolve the dusty structures around AGN.

2 Observations

So far six AGN have been successfully observed with MIDI. These are the well-known galaxies NGC 1068 and Circinus, which are "bright" ($F_N > 1$ Jy) in the N band, as well as the fainter ($F_N \leq 1$ Jy) galaxies Centaurus A, NGC 3783, Mrk 1239 and MCG -05-23-016. The targets are the brightest and nearest AGN accessible from Paranal. Nevertheless, they are so faint that most of them have to be observed at the sensitivity limit of MIDI. All of the targets were observed in "HIGH_SENS" mode using either science demonstration time (SDT) or guaranteed time observations (GTO), except for NGC 3783, which was observed in open time.

The main limiting factor for the observations is currently the acquisition procedure: the two beams coming from the telescopes need to be iteratively recentered in order to achieve a good overlap of the two beams (for more general aspects of the MIDI instrument and details of the observation procedure see the contribution by Olivier Chesneau). As an example, the acquisition images for a calibrator (top row) and Mrk 1239 (bottom row) are shown in figure 1.

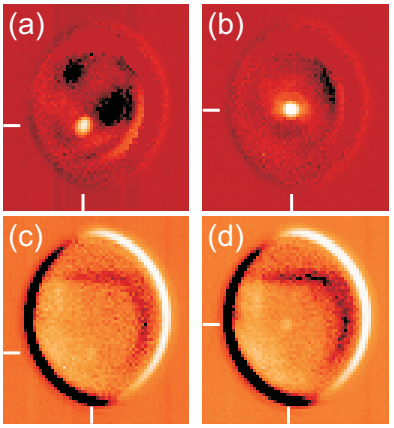

Fig. 1. Examples for aquisition images of the calibrator HD 120404 (flux $F \sim 10.0\,\mathrm{Jy}$) and Mrk 1239 (flux $F \sim 0.6\,\mathrm{Jy}$). All images were observed with the N8.7 filter and $DIT = 4\,\mathrm{ms}$. The source position is indicated by the white bars. (a) – first acquisition of HD 120404 ($NDIT = 1000$), (b) – final acquisition frame of HD 120404 before fringe tracking ($NDIT = 1000$), (c) – first acquisition of Mrk 1239 ($NDIT = 8000$) and (d) final acquisition of Mrk 1239 ($NDIT = 12000$).

The left frames respectively show the first acquisition frame, the right ones are the frames after the alignment process, before the fringe search starts. These images clearly demonstrate the low flux of the AGN compared to that of the calibrator. For the AGN, the number of individual exposures had to be increased from the default value of $NDIT = 1000$ to 12000 in order to produce the images shown. Still the source has a very low signal to noise ratio, simply due to its faintness. Additional emission from the VLTI delay line tunnels (due to the lack of variable curvature mirrors, VCMs) and the residuals from the background subtraction (using chopping) make the detection of such sources even more difficult. By consequence, the acquisition process takes considerably longer than for a bright source.

Once the acquisition succeeded, the subsequent fringe search and track have been straight forward for all AGN observed. This is due to the fact that the two inverse interferometric signals are subtracted in order to determine the current optical path difference (OPD), leading to an effective elimination of the uncorrelated sky background. The ensuing observation of the photometry, however, is delicate again. Here similar problems as for the acquisition appear. By consequence, the photometry has large errors and it is the limiting factor for the accuracy of the determination of the visibility. By way of example, the photometry of Centaurus A is shown in figure 2. The lower frames are the final sky subtracted detector frames from the two telescopes using the chopped raw data: beam A (top) and beam B (bottom). The continuous curves in the plot show the flux inside a boxcar mask, indicated by the thick marks on the detector frames. The dip between columns 100 and 110 on the detector ($\sim 9.7\,\mu\mathrm{m}$) is caused by atmospheric ozone absorption. The dashed lines show the remaining sky background in two bands above and below the source spec-

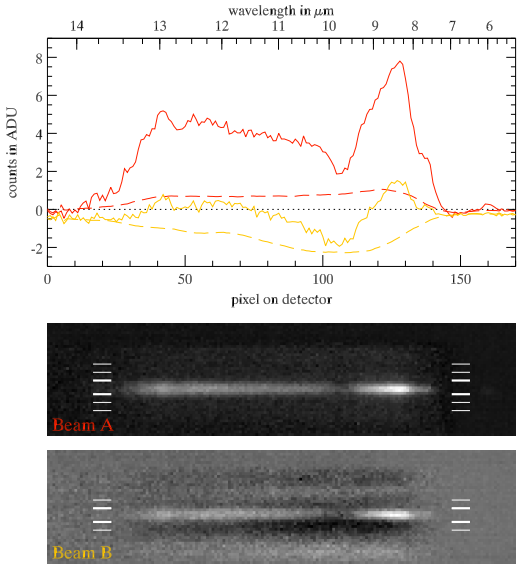

Fig. 2. Photometry of Centaurus A showing imperfect background subtraction through chopping. The plot shows the integrated flux in a boxcar mask (marked by two thick lines on the detector frames, below) from telescope A (red) and telescope B (orange). The flux level determined in two extra sky bands above and below the object (thin lines on the detector frames) are shown as dashed lines. For beam B the sky bands had to be changed so that they adjoin the area where the flux is extracted.

trum (thin marks on the detector frames). In beam B, the variations of the background residual lead to a negative flux, which can only be corrected by adjusting the position of the sky bands: in this case, the sky bands have to be moved closer to the spectrum, so that they lie directly next to the area used to extract the flux. A significant amount of data on AGN has such defects. For weak sources, it is hence advisable to not use the visibility as the final result of the observations but the correlated flux, which can be determined directly without using the photometry.

3 Data reduction

The data reduction for AGN was performed exclusively by the coherent visibility estimation with the software package EWS (Expert Work Station), written by Walter Jaffe. The advantage of using the coherent visibility estimation is twofold: firstly, it is currently possible to obtain results for much lower signal to noise ratio than with the coherent package MIA and, secondly, it also extracts the differential phase from the data. I will therefore give a very brief overview over this data reduction package. The software is part of the MIA+EWS

package, which can be downloaded from the Sterrewacht Leiden [1] . A detailed description of the coherent method can be found in Jaffe et al. (2004). The full data reduction possibilities are discussed in the contribution by Olivier Chesneau.

The data reduction in EWS is perfomed in a pipeline type fashion: first, a fixed mask is applied to the two oppositely phased interferograms, which are then collapsed to form two one dimensional interferograms. These are then subtracted one from the other with the result of doubling the signal while removing most of the background. As the fringes vary rapidly in time due to the scanning of the MIDI internal mirrors, a boxcar smoothing in temporal direction is performed to further remove the background. In the following two steps, the known instrumental OPD and the atmospheric delay are removed. The latter is estimated from the group delay. Additionally, a constant phase shift induced by the varying index of refraction of water vapour is estimated and also removed. After rejecting frames with too low or too high optical path differences, the remaining data are averaged coherently so as to yield the raw correlated flux.

To determine the raw total flux of the target, first standard data reduction methods for chopped data are applied to the photometric data: the sky frames are subtracted from the object frames. As this does not lead to a satisfactory sky subtraction (see previous section), two bands on the detector frame, one above the target position and one below, are used to subtract an additional sky estimate, which is wavelength dependent. The data are then compressed and averaged to a one-dimensional photometry.

Dividing the correlated flux by the photometry yields the raw visibility. To calibrate this for instrumental and atmospheric visibility losses, the same procedure has to be applied to a calibrator star. The calibrated visibility is then obtained by dividing the visibility of the object by that of the calibrator. As mentioned before, it is often advisable to use the correlated flux instead of the visibility. Here, EWS offers the option to calibrate the correlated fluxes directly using the correlated flux of the calibrator only, without taking the photometric data into account at all.

[1] `http://www.strw.leidenuniv.nl/~nevec/MIDI/index.html`

(a)

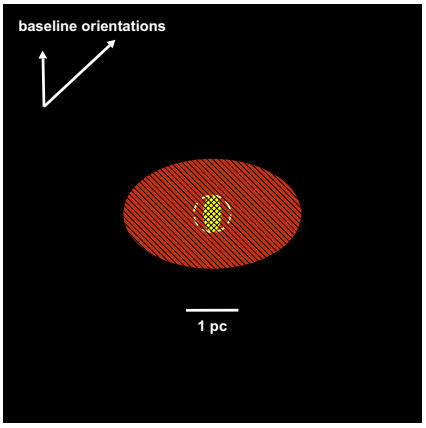

(b)

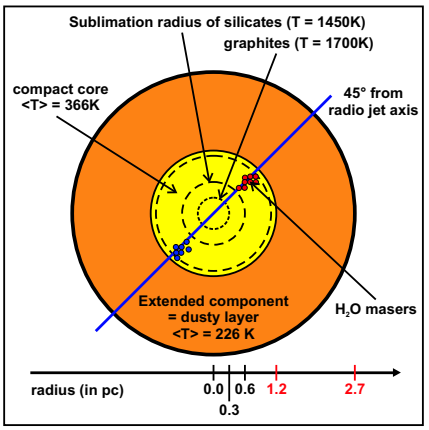

Fig. 3. Sketches of the models used to explain the interferometric measurements of NGC 1068 (identical scale). (a) Model by Jaffe et al. (2004) consisting of two Gaussian black body emitters: a hot ($T > 800\,\mathrm{K}$) compact component is embedded in a warm ($T = 320\,\mathrm{K}$) component, which is elongated perpendicularly to the nuclear radio jet. (b) Model by Poncelet et al. (2006). Here, a hot uniform disc emitting black body radiation at $T = 370\,\mathrm{K}$ is surrounded by a cooler and larger disc with $T = 230\,\mathrm{K}$.

4 Results

4.1 NGC 1068

The first object observed was the famous active galaxy NGC 1068. This galaxy, located at a distance of 14 Mpc, is the most extensively studied Seyfert 2 galaxy due to its proximity and its brightness. Its polarised optical spectrum is similar to that of a type 1 object, which led Antonucci & Miller (1985) to the conclusion that it contains a hidden Seyfert 1 nucleus. This in turn originally gave rise to the picture of the unified scheme described in section 1.

NGC 1068 was observed with MIDI using two baseline configurations, that is, essentially two visibility points were measured. The data was analysed twice: a first investigation is presented in Jaffe et al. (2004), followed by a more detailed one in Poncelet et al. (2006). Sketches of the models put forward in these two papers are shown in figure 3. The relatively low visibilities of $V < 20\%$ measured with MIDI show that the core of NGC 1068 is well resolved in the MIR.

Jaffe et al. (2004) modelled the MIDI data by a two component model that is symmetric with respect to the north-south-oriented source axis, which is defined by the inner radio jet. Each of the two components consists of a black body emitter at a specific temperature with an elliptical Gaussian brightness distribution. In order to reproduce the dust absorption feature, silicate absorption of different strength for the two components was introduced. The

absorption profile was derived from Infrared Satellite Observatory (ISO) observations of the centre of our Galaxy (Kemper et al. (2004)). The first, smaller component in this model is hot ($T > 800\,\mathrm{K}$) and compact. Its length along the source axis is resolved and well constrained to 0.7 pc. The interferometric measurement only sets an upper limit of 1 pc to its orthogonal width. The second component is warm and well-resolved with a best-fit temperature of $T = 320\,\mathrm{K}$. The observations with the two baselines constrain the size of this component to $2.1 \times 3.4\,\mathrm{pc}$ with the larger extent perpendicular to the jet axis (see figure 3a). The silicate absorption feature around $10\,\mu\mathrm{m}$ is found to be much more pronounced in the interferometric spectra than in the total spectrum. By consequence, the extended component has an optical depth of the silicate absorption of 0.3, while the hot component is exposed to an additional absorption with a depth of 1.8. Furthermore, the shape of the absorption profile in the correlated fluxes seem to require special dust properties in the innermost 2 pc around the nucleus of NGC 1068.

Poncelet et al. (2006) applied different basic models with an increasing complexity to the data in order to fit both the interferometric and the spectral data. Ultimately, a two component model with two concentric spherical components is chosen. These components consist of uniform discs emitting black body radiation. The inner compact component is found to have a radius of about 1.2 pc and a temperature of about 370 K, and the outer component extends up to 2.9 pc from the nucleus and has an average temperature of about 230 K (see figure 3b). In this model, which did not include an a priori assumption about the nature of the silicate absorption, the evolution of the optical depth of the absorption feature across the N band could be extracted. Although this parameter is model-dependent, its shape is found to be characteristic of amorphous silicate grains.

Although the two analyses are based on the same data set, they show significant discrepancies. The differences start with the different flux levels obtained for the calibrated data (which differ up to a factor of 2, most likely due to differing calibration), they include the choice of the modelling procedure and end with the different results obtained. This shows that the interpretation of the interferometric data for even the brightest extragalactic source is not trivial. In any case it is reassuring that both models recover a hot component with a size of $\sim 1\,\mathrm{pc}$ embedded in a larger and cooler component of $\sim 3\,\mathrm{pc}$. This confirms the general picture of a geometrically thick dust distribution at the nucleus of this galaxy. Both analyses also agree on the fact that amorphous silicate dust is responsible for most of the silicate absorption feature. The differences appearing at the next level of detail show that the interferometric data is degenerate and that more observations are needed to resolve the details of the morphology of the dust distribution. Indeed, a follow-up programme was initiated and the data is currently being analysed.

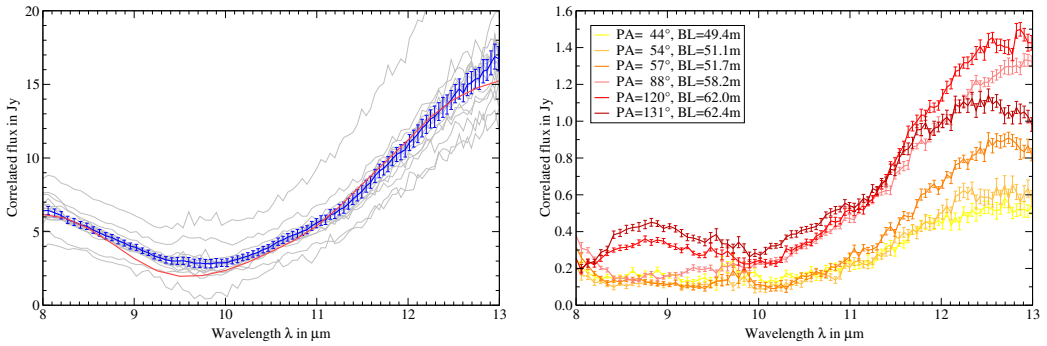

Fig. 4. (a) Individual photometries of the Circinus nucleus in the N band (light gray), averaged photometry (blue) and total flux of the model (red). (b) Correlated fluxes as observed during the night of 2005-02-28. Primarily the baseline angle changed, while the projected baseline length stayed roughly the same. From the dramatic change in the correlated fluxes, direct implications for the morphology can be derived: the source is considerably more extended in the direction of $PA \sim 50°$ than in the direction of $PA \sim 130°$.

4.2 Circinus

The Circinus galaxy is a highly inclined ($\sim 65°$) spiral galaxy harbouring a Seyfert type 2 active nucleus as well as a circumnuclear starburst. At about 4 Mpc distance ($1'' \sim 20$ pc, Freeman et al. (1977)), the galaxy is even closer than NGC 1068, albeit not as bright.

So far a total of 21 visibility points were obtained with MIDI. Figure 4a shows the calibrated total flux F_{tot} of Circinus (thick blue line). The broad absorption feature dominating most of the spectrum is due to silicate absorption. No evidence for any line emission or emission of Polycyclic Aromatic Hydrocarbons (PAH), as observed at greater distances from the nucleus, e.g. by Roche et al. (2006), is seen.

For all baselines observed, the correlated flux F_{cor} is much smaller than the total flux ($F_{cor} \ll F_{tot}$), indicating that the emission region is well resolved with the interferometric resolution of $\lambda/2B \leq 40$ mas. For example, the correlated fluxes obtained on February 28^{th}, 2005, are shown in figure 4b. During these observations, the projected baseline length increased only by a minor factor from 50 to 60 m, while the position angle underwent a major change from 44 to 131°. An increase of the correlated flux can clearly be observed while the position angle increases. This can be interpreted directly as a change of size of the emitting source: at position angles of 44 to 57° the correlated flux is low, i.e. the emission is extended, while at angles of 120 and 131° the correlated flux is higher, i.e. the emission is less resolved. This is a direct and completely model indpendent evidence for an elongated dust structure perpendicular to the ionisation cone and outflow (position angle $-50°$ and opening angle $\sim 90°$)

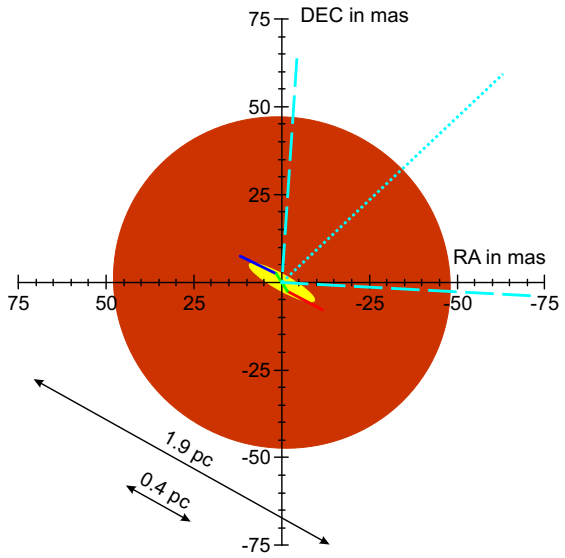

parameter	best fit value
$FWHM_1$	21.1
a_1/b_1	0.21
τ_1	1.18
T_1	333.7
f_1	1.0
$FWHM_2$	96.7
a_2/b_2	0.97
τ_2	2.22
T_2	298.4
f_2	0.20
α	60.9
$\bar{\chi}^2$ (451 d.o.f.)	36.9

Fig. 5. Sketch and best fit parameters of the two component model for Circinus. A highly elongated hot emission region (yellow) is surrounded by an extended, almost round and cooler emission region (brown). At the centre, the locus of H_2O maser emitters in a disk from Greenhill et al. (2003) is overplotted. The orientation of the visible ionisation cone is outlined by the light blue, dashed lines. The parameters fitted are: $FWHM$ – full width at half maximum (in mas), a/b – axis ratio, T – temperature (in K) and f – filling factor, τ – optical depth of the silicate absorption for each of the two components and α – position angle for both components.

in Circinus.

Even though the coverage is high for long baseline infrared interferometry, it is insufficient to attempt any image reconstruction. Therefore Tristram et al. (2007) used a simple model consisting of two black body Gaussian emitters with silicate absorption to explain the data. The silicate absorption profile for interstellar dust from Kemper et al. (2004) is found to be sufficient to describe the absorption feature observed with MIDI, both for the total flux as well as for the correlated fluxes. The two component black body model has 11 free parameters, which are listed in figure 5 with their best fit values. The figure also contains a sketch of the best fit model.

The small hot component is found to have a FWHM of 21 mas (~ 0.4 pc at the distance of Circinus). The component is highly ellipsoidal; it has a temperature of 330 K and the same size and position angle as the warped maser disc found by Greenhill et al. (2003) (see figure 5). The second component is significantly larger, reflecting the fact that a large part of the flux ($\sim 90\%$) is resolved by

the interferometer. The component has a FWHM of 97 mas, which corresponds to 1.9 pc. It has a very small ellipticity and a temperature of less than 300 K. It is a grey body with a filling factor of 0.2, that is, the intensity is only a fifth of that of a pure black body. The 330 K for the inner component are considered as the lower limit for the highest dust temperature and the 300 K as the upper limit for the cool component. The data shows no indications for a truly hot component with temperatures $T > 1000$ K, i.e. close to the sublimation temperature of the dust. Clearly, there is a temperature gradient from the inside to the outside, indicating that the dust is heated by the nuclear source.

The model was kept as simple as possible in order to extract the overall properties of the emitting source. Hence the comparison with the data shows significant discrepancies. However, the general behaviour is reproduced well and the deviations from the model may be due to the substructure of the source, e.g. due to clumpiness.

4.3 Centaurus A

Centaurus A (NGC 5128) is the closest active galaxy at a distance of only 3.8 Mpc (1 pc $\sim$ 50 mas, Rejkuba (2004)). It is an elliptical galaxy undergoing late stages of a merger event with a spiral galaxy.

The results of MIDI observations, presented in Meisenheimer et al. (2007), are summarised in figure 6a, which shows the total flux and the correlated fluxes of the two baseline sets observed. Similar to the previous two objects, most of the spectral region observed is affected by the very broad silicate absorption feature. Its depth is identical in the correlated and in the total flux, indicating that both the core and extended components suffer the same extinction. The [NeII] emission line at 12.9 μm is clearly detected at the edge of the total spectra, but it is not present in any of the correlated flux spectra. The interferometric observations reveal the existence of two components in the inner parsec of Centaurus A: a resolved component, the "disc", which is most extended along a position angle of $\sim 110°$ and an unresolved "core".

The disc is hence roughly orientated perpendicular to the parsec scale radio jet. The decrease in visibility towards longer wavelengths indicates that the extended emission has a spectrum which rises steeply between 9 and 13 μm as expected for emission from thermal dust at temperatures $T < 300$ K. The size of the disk is poorly defined by the observations but needs to be > 30 mas (~ 0.57 pc) at 13 μm, in order to be consistent with the simple two-component model.

In order to understand the nature of the unresolved core emission, the mid

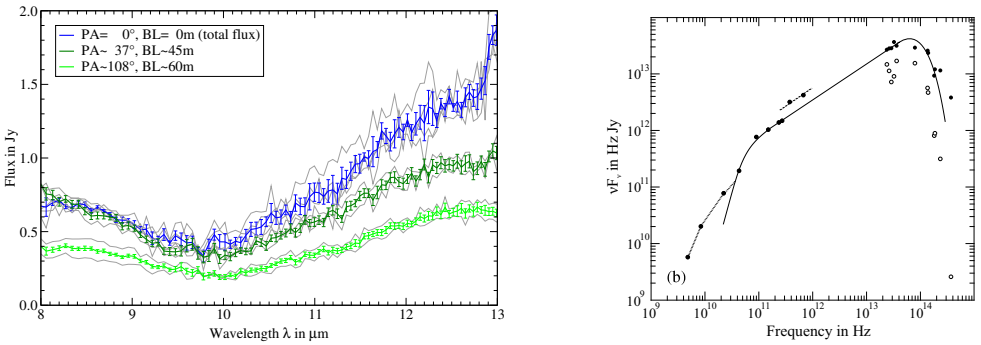

Fig. 6. (a) Total flux (blue) and correlated fluxes (green) for Centaurus A. Two baseline sets (consisting of two visibility points each) were observed. (b) Overall spectrum of the core of Centaurus A. Open circles show observed flux values, filled dots are corrected for foreground extinction. The synchrotron spectrum (solid line) shows an optically thin power-law $F\nu \sim \nu^{-0.36}$.

infrared photometry was supplemented by measurements at lower and higher frequencies, using VLBA, millimeter and near infrared data (see figure 6b). Both the mm-data and the core flux in the MIDI range can be nicely fitted by an optically thin power-law spectrum. This leads to the conclusion that the core emission is dominated by non-thermal synchrotron radiation. This means that, in Centaurus A, the MIR emission is dominated by an unresolved synchrotron core making up between 60% (at 13 μm) and 80% (at 8 μm) of the nuclear MIR flux. The size of this core most likely is $R_c \sim 0.01$ pc, as derived from VLBI observations at 43 GHz.

4.4 Faint AGN

The sensitivity of MIDI is better than initially predicted, so that two fainter AGN, MCG-05-23-01 and Mrk 1239, could be successfully observed in GTO. Only one UV point for each object was obtained in order to check the feasibility of observations. A further target, NGC 3783, was observed in open time. MCG -05-23-01 is a Seyfert 2 galaxy at a distance of approximately 40 Mpc. It might also show a silicate absorption feature. Mrk 1239 and NGC 3783, however, are the only Seyfert 1 galaxies observed with MIDI. They are located at a distance of about 90 Mpc and 45 Mpc, respectively. Both have flat spectra in the MIR. The correlated fluxes of these sources are consistent with marginally or even unresolved objects ($F_{cor} \lessapprox F_{tot}$). The flux level of Mrk 1239 is 400 mJy and that of MCG-05-23-01 only 300 mJy.

5 Conclusions

Considering the obvious success of MIDI, it is planned to observe more AGN shortly. With two to three visibility points the size of the dust emission can be estimated for a number of objects. Simultaneously the investigations of the targets already observed will be continued. The current studies of NGC 1068 and Circinus show the high degree of ambiguity in the data consisting of several measurements. The inability of a simple model to explain these data sets shows that the physical properties and the distribution of the dust around the AGN are more complicated than suggested in the simple unified scheme. More complete UV coverages must be obtained with the final goal to directly image the dust distribution. In this respect, the puzzle is not fully resolved yet.

References

Antonucci, R. R. J. and Miller, J. S. 1985, *ApJ* 297, p. 621-632
Freeman, K. C. et al. 1977, *A&A* 55, p. 445-458
Greenhill, L. J. et al. 2003, *ApJ* 590, p. 162-173
Jaffe, W. et al. 2004, *Nature* 429, p. 47-49
Kemper, F., Vriend, W. J., Tielens, A. G. G. M. 2004, *ApJ* 609, p. 826-837
Meisenheimer, K. et al. 2007, submitted to *A&A*
Poncelet, A., Perrin, G. and Sol, H. 2006, *A&A* 450, p. 483-494
Rejkuba, M. 2004, *A&A* 413, p. 903-912
Roche, P. F. et al. 2006, *MNRAS* 367, p. 1689-1698
Tristram, K. R. W. et al. 2007, submitted to *A&A*